Heliyon 9 (2023) e16631

Contents lists available at ScienceDirect

Heliyon

journal homepage: www.cell.com/heliyon

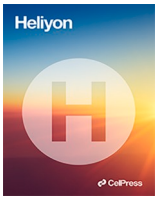

Research article

Mechanism of new optimized Sheng-Mai-San Formula to regulate cardiomyocyte apoptosis through NMDAR pathway

Yazhu Hou [a,1], Zixun He [a,c,1], Yixiao Han [d], Tongyan Zhang [b], Shuai Wang [a], Xianliang Wang [a,**], Jingyuan Mao [a,*]

[a] *Department of Cardiovascular Diseases, First Teaching Hospital of Tianjin University of Traditional Chinese Medicine, National Clinical Research Center for Chinese Medicine Acupuncture and Moxibustion, Tianjin 300381, China*
[b] *Second Affiliated Hospital of Tianjin University of Traditional Chinese Medicine, Tianjin 300150, China*
[c] *Tianjin University of Traditional Chinese Medicine, Tianjin 301617, China*
[d] *Shenzhen Traditional Chinese Medicine Hospital, Shenzhen, China*

ARTICLE INFO

Keywords:
NO-SMS
NMDAR pathway
Cardiovascular disease
Cardiomyocyte apoptosis

ABSTRACT

Background and objectives: Ischemic heart failure (HF) has become a disease that seriously endangers people's life and health. As a herbal formula widely used in clinical practice, new optimized Sheng-Mai-San (NO-SMS) has been shown to be significantly effective in improving cardiac function, increasing exercise tolerance, and slowing the progression of myocardial fibrosis in heart failure patients in multi-center clinical studies in various regions of China. In our previous pharmacodynamic and toxicological studies, we found that a medium-dose formulation (8.1 g of raw drug/kg) was the most effective in the treatment of heart failure, but its mechanism of action is still being investigated. The present study is exploring its relationship with cardiomyocyte apoptosis.

Materials and methods: We investigated and verified this through two parts of experiments, in vivo and in vitro. Firstly, we prepared male SD rats with heart failure models by ligating the left anterior descending branch of the coronary artery (EF $\leq$ 50%), which were treated with NO-SMS Formula (8.1 g of raw drug/kg/d), Ifenprodil (5.4 mg/kg/d) or Enalapril (0.9 mg/kg/d) prepared suspensions by gavage for 4 weeks. The cardiac and structural changes were evaluated by echocardiography, H&E, and MASSON staining. The apoptosis of cardiomyocytes in each group was detected by Western blot, qRT-PCR, and ELISA. In vitro cell experiments include H9c2 cardiomyocyte injury induced by H_2O_2 and NMDA respectively, and the groups were incubated with NO-SMS and Ifenprodil-containing serum for 24 h. Apoptosis was detected by Annexin V-FITC/PI double-staining method, and the rest of the assays were consistent with the in vivo experiments.

Results: Compared with the model group, the NO-SMS formula group and the Ifenprodil group could significantly improve cardiac function, delay myocardial fibrosis, reduce the expression of pro-apoptotic proteins, mRNA, and the concentration levels of Ca^{2+} and ROS in heart failure rats and H9c2 cardiomyocytes with H_2O_2 and NMDA-induced injury, which could significantly reduce the apoptosis rate of damaged cardiomyocytes and effectively inhibit the apoptosis of cardiomyocytes.

* Corresponding author.
** Corresponding author.
E-mail addresses: xlwang1981@126.com (X. Wang), jymao@126.com (J. Mao).
[1] Contributed to this article equally.

https://doi.org/10.1016/j.heliyon.2023.e16631
Received 11 March 2023; Received in revised form 21 May 2023; Accepted 23 May 2023
Available online 29 May 2023

Conclusion: NO-SMS Formula improved cardiac function, inhibited ventricular remodeling and cardiomyocyte apoptosis in HF rats, and its mechanism may be related to the regulation of the NMDAR signaling pathway, inhibition of large intracellular Ca^{2+} inward flow, and ROS production in cardiomyocytes.

1. Introduction

In developed countries, HF remains the leading cause of death. Despite our significant medical advances, including effective coronary interventions for patients with acute myocardial infarction, the number of HF patients continues to increase [1,2]. HF is a complex clinical syndrome with multiple risk factors and a complex condition [3–6]. With the advancement of basic research and evidence-based medicine, cardiomyocyte apoptosis has gradually become an important pathogenic mechanism of HF [7,8]. The increased level of apoptosis leads to a cumulative loss of cardiomyocytes, resulting in progressive myocardial dysfunction and further progression to ventricular remodeling, and then which leads to HF. Therefore, inhibition of cardiomyocyte apoptosis can be an effective strategy for the treatment of HF [9].

The N-methyl-D-aspartate receptor (NMDAR) is an important ionotropic glutamate receptor that is found mainly in peripheral tissues such as the heart and vascular endothelium in addition to the central nervous system. Some studies [10–14] have shown that the NMDAR signaling pathway is activated by the necessary conditions such as the synergistic action of glutamate (Glu) and glycine (Gly) and cell membrane depolarization [15–18]. When the myocardial injury occurred, the transport and metabolism of glutamate (Glu) and glycine (Gly) become impaired and accumulate outside the cell membrane, binding to NMDAR, leading to Ca^{2+} overload [17, 19–21], which makes the calcium homeostasis in the endoplasmic reticulum imbalanced and endoplasmic reticulum stress occurred, leading to apoptosis [14,22], irreversible myocardial damage, and eventually heart failure [23–25].

New Optimized Sheng-Mai-San (NO-SMS) Formula, which is derived from the Sheng-Mai-San formula, has the effect of invigorating Qi, activating blood circulation, and promoting water circulation. Its active ingredients may consist of isorhamnetin, quercetin, kaempferol, tanshinone IIA, etc [26]. The formula is based on the research of evidence-based medicine, with appropriate additions and reductions. In many randomized controlled clinical trials conducted in different regions of China, including Tianjin [27], Shandong [28], Guangdong [29], and Beijing [30], we found that the combination of New Optimized Sheng-Mai-San Formula and conventional treatment had a more significant improvement in patient's clinical symptoms, exercise tolerance, and cardiac ejection fraction than conventional heart failure treatment alone. But there is a lack of exact research on its specific drug mechanism of action. In our previous literature study [31], we explored that the mechanism of action may be related to the inhibition of NMDAR pathway activation and thus apoptosis. Therefore we aimed to investigate whether NO-SMS formula could inhibit the activation of the NMDAR signaling pathway, thereby inhibiting apoptosis, improving cardiac function, and thus treating heart failure.

2. Materials and methods

2.1. Experimental animals

This study was approved by the Laboratory Animal Ethics Committee of the Institute of Chinese Academy of Sciences (ethics No. IRM-DWLL-2020109). This experiment complies with the provisions of the British Animals (Scientific Procedures) Act 1986. We used specific pathogen-free (SPF) grade male SD rats (Beijing SiPeifu Biotechnology Co., Ltd. (Beijing, China), animal production license No. SCXK (Beijing) 2019-0010) routinely housed in the animal house of the Institute of Radiological Medicine, Chinese Academy of Medical Sciences (SYXK (Tianjin) 2019-0002). After 7 days of acclimatization feeding, 160 qualified rats weighing 200–220 g and of similar age were selected.

2.2. Materials and reagents

During our experiments on the pharmacodynamics and toxicology of NO-SMS formula, we found that the efficacy of using the medium-dose group (8.1 g of raw drug/kg) to improve the symptoms of heart failure was superior to that of the high-dose group (16.2 g of raw drug/kg) and the low-dose group (4.05 g of raw drug/kg) in the rat experiments, and also in published basic studies on dose [32–34], all verified the effectiveness of the medium dose, so in our current study, we mainly used the medium dose administration to investigate the relevant mechanism of action behind its clinical effectiveness.

NO-SMS Formula Composition: 10 g of *Astragalus membranaceus* (Fisch.) Bge, 10 g of *Codonopsis pilosula* (Franch.) Nannf, 10 g of *Acanthopanax gracilistylus* W.W.Smith, 10 g of Turtle Shell, 6 g of *Draba nemorosa* L, 10 g of *Poria cocos* (Schw.) Wolf, 10 g of *Ophiopogon japonicus (Linn. f.) Ker-Gawl,* 6 g of *Citrus aurantium* L, 10 g of *Salvia miltiorrhiza* Bunge, 10 times concentrated granules prepared from the above nine herbs by boiling and extracting, vacuum drying, crushing into powder, mixing and packing. The above particles were configured with 0.5% sodium carboxymethyl cellulose to form a suspension of 0.81 g/ml (First Teaching Hospital of Tianjin University of Traditional Chinese Medicine, China); Enalapril (0.9 mg/kg) (Jiangsu Pharmaceutical Co., Ltd, product lot No.20052311, China) was configured with 0.5% sodium carboxymethyl cellulose to form a suspension of 0.81 g/ml; Ifenprodil (5.4 mg/kg) (MCE, product lot No. 46903, USA) was configured with 0.5% sodium carboxymethyl cellulose to form a suspension of 0.54 g/ml.

Drug-containing serum preparation: Thirty male rats were randomly divided into blank, NO-SMS formula, and Ifenprodil groups.

The NO-SMS formula group and the Effendiel group were gavaged with the corresponding drugs in a volume of 1 ml/100 g. The blank group was gavaged with the same volume of solvent (0.5% CMC-Na). The drugs were administered continuously for 7 d, Qd. After the last dose of 0 min, 30min, 60min, 90min, 120min and 180min, blood was taken from the abdominal aorta, left to stand, and centrifuged at 3500r min^{-1} centrifuged for 15min, and the serum containing the drug in the same group was combined and mixed to reduce individual differences between animals, divided, sealed with sealing film, and stored at −80 °C. The serum was inactivated in a water bath at 56 °C for 30min and de-bacterized through a 0.22 μm microporous filter membrane before use.

Other Materials: NMDA (MCE, product lot No. 87585, USA); BCA Protein Assay Kit (Thermo, Meridian Rd; Rockford, IL61101, USA); HP Total RNA Assay Kit (Omega Bio-Tek, Norcross, GA); HiScript® Q RT SuperMix Kit (Vazyme biotech co; Ltd); SYBR qPCR Master Mix (Vazyme biotech co; Ltd); 0.5% sodium carboxymethyl cellulose (0.5% CMC-Na).

2.3. Model preparation and grouping

We selected 160 normal male SD rats that met the requirements to prepare the HF model by ligating the anterior descending branch of the coronary artery. Echocardiography was performed at 6 weeks after surgery to assess rat modeling, and rats with EF $\leq$ 50% were used as a marker of successful heart failure modeling. The rats that did not meet the requirements were excluded, and then 32 rats that met the criteria were randomly and equally divided into 4 groups: Model group, NO-SMS group, Ifenprodil group, and Enalapril group, and another 8 rats were set as Sham group (without coronary artery ligation). The Sham and Model groups were given blank solvent (0.5% CMC-Na), and the remaining groups were given the corresponding drugs, 1 ml/100 g/d, for 4 weeks.

2.4. Echocardiography

After 4 weeks of administration, the anesthetized rats were fixed dorsally on rat plates and maintained in low-dose anesthesia by connecting an isoflurane anesthesia system. An appropriate amount of coupling agent was applied to the precordial region and the Vevo 3100 small animal ultrasound instrument (Visual Sonics, Canada) was turned on and the MS-250 probe was positioned to the long-axis cross-section at the level of the papillary muscles. Three consecutive cardiac cycle measurements were performed to calculate the long-axis ejection fraction (EF/%) and short-axis shortening fraction (FS/%) of the left ventricle (mean values were taken). The body temperature of the animals was maintained at 37 °C during the procedure.

2.5. Pathological tissue observation

The rats were executed 24 h after the final administration, and the hearts were fixed using 4% paraformaldehyde solution and cut into 4-μm wax strips after dehydration and transparency and immersion wax embedding, followed by hematoxylin-eosin (HE) staining and MASSON staining of the sections to observe the pathological changes and fibrosis level around the myocardial infarction area under a 400 × light microscope and to determine the collagen area of the tissue.

2.6. TUNEL staining

The TUNEL staining was used to detect apoptosis, and the operation was performed according to the kit instructions. The green fluorescent cell nuclei were used as the uniform standard for positive cells in all photos, and the DAPI blue cell nuclei with the same markers were selected as the total cells. The Image software was used to calculate and analyze the number of positive cells and the total number of cells in each photo, and the percentage of positive cells (positive cells/total cells*100) was calculated as the apoptosis rate (%).

2.7. Cell culture and grouping

Rat cardiomyocytes (H9c2) were added to DMEM complete medium containing 10% fetal bovine serum (Biological Industries, Israel) and 1% penicillin-streptomycin solution (Service) and incubated at 37 °C in a 5% CO_2 incubator (Thermo Scientific, Germany) for 1 h. To observe the cell recovery status, the obtained cells were repeatedly and gently washed with PBS 3 times and then added to the complete medium for culture, and the cells in the growth phase and good condition were taken for aseptic freezing.

Cultured H9c2 cardiomyocytes were placed in DMEM medium in random groups and H_2O_2/NMDA was added separately for in

Table 1
The sequence of forward and reverse primer.

	Forward (5′-3′)	Reverse (3′-5′)
GAPDH	CTGGAGAAACCTGCCAAGTATG	GGTGGAAGAATGGGAGTTGCT
Caspase-3	CTGGACTGCGGTATTGAGACA	CGGGTGCGGTAGAGTAAGC
Caspase-9	CCACTGCCTCATCATCAACAAC	GCCGTGACCATTTTCTTAGCAG
Caspase-12	GGAGGTAAATGTTGGAGTGGC	TTGTTGCAGATGATGAGGGC
Cyt-c	TTGTTGCAGATGATGAGGGC	GGTCTGCCCTTTCTCCCTTCT
Bax	TGAACTGGACAACAACATGGAG	AGCAAAGTAGAAAAGGGCAACC
Bcl-2	TTGTGGCCTTCTTTGAGTTCG	GCATCCCAGCCTCCGTTAT

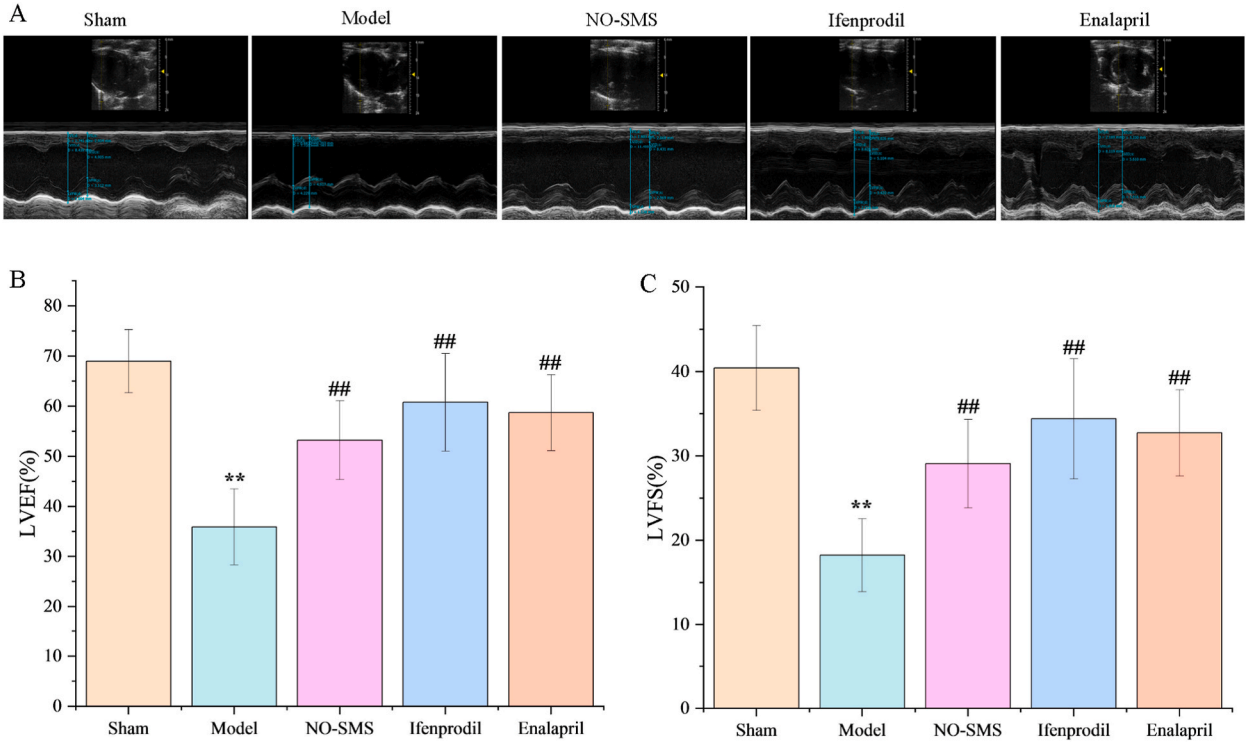

Fig. 1. Left heart function of rats in each group after drug administration. M-mode ultrasound images of rats in each group after 4 weeks of treatment (A); LVEF values of rats in each group after 4 weeks of treatment (B); LVFS values of rats in each group after 4 weeks of treatment (C). (Compared with Sham, $^{**}P < 0.01$; compared with Model, $^{\#\#}P < 0.01$).

vitro induction of injury: (1) H_2O_2 group: final concentration of 400 μM H_2O_2 + 10% of 0.5% CMC-Na blank serum; (2) H_2O_2+NO-SMS group: final concentration of 400 μM H_2O_2 + 10% of NO-SMS-containing serum; (3) H_2O_2+Ifenprodil group: final concentration of 400 μM H_2O_2 + 10% of Ifenprodil-containing serum; (4) NMDA group: final concentration of 10^{-2} M NMDA + 10% of 0.5% CMC-Na blank serum; (5)NMDA + NO-SMS group: final concentration of 10^{-2} M NMDA + 10% of NO-SMS-containing serum; (6) NMDA + Ifenprodil group: final concentration of 10^{-2} M NMDA +10% Ifenprodil-containing serum; (7) Control group: 10% of 0.5% CMC-Na blank serum. The drug serum was prepared by randomly grouping 30 SD rats, administered in a volume of 1 ml/100 g/d for 7 days, and blood was collected from the abdominal aorta, centrifuged at 3500 rpm for 15 min, and stored at −80 °C. The serum was decontaminated by a 0.22 μm microporous membrane in a water bath at 56 °C for 30 min before use.

2.8. Apoptosis detection by flow cytometry

After each group of cells was treated with drug-containing serum for 24 h, they were collected in EP tubes to ensure that the number of cells in each EP tube was higher than 1 × 10^6/ml, and then they were washed with PBS, centrifuged at 300×*g* min-1 for 10min, added 1 × Binding Buffer to suspend the cells, centrifuged at 300×*g* min^{-1} for 10min, discarded the liquid, added 1 × Binding Buffer to suspend the cells, added 5 μL Annexin V-FITC reagent shaking lightly at room temperature for 10min, added 5 μL PI reagent, incubating for 5min at room temperature without light, added PBS to 500 μL of liquid, mixed well and measured the apoptosis rate. On the flow cytometry scatter plot, Annexin V-FITC is the horizontal axis and PI is the vertical axis, the lower left quadrant shows normal cells, the lower right quadrant shows early apoptotic cells, and the upper right quadrant shows intermediate to late apoptotic cells with necrotic cells.

2.9. ELISA for Ca^{2+} and ROS concentration

Myocardial tissue (30 mg) of SD rats after four weeks of drug intervention and H9c2 cardiomyocytes after 24 h of drug intervention were homogenized and the supernatant was taken, followed by setting up blank wells, standard wells, and sample wells according to the instructions, added 50 μL diluent、standards of different concentrations and samples to be tested, respectively, and then added 100 μL of labeled antibodies to each well, washed the plate with washing solution, added substrate A and B and termination solution, and placed it at 450 nm to determine the OD value.

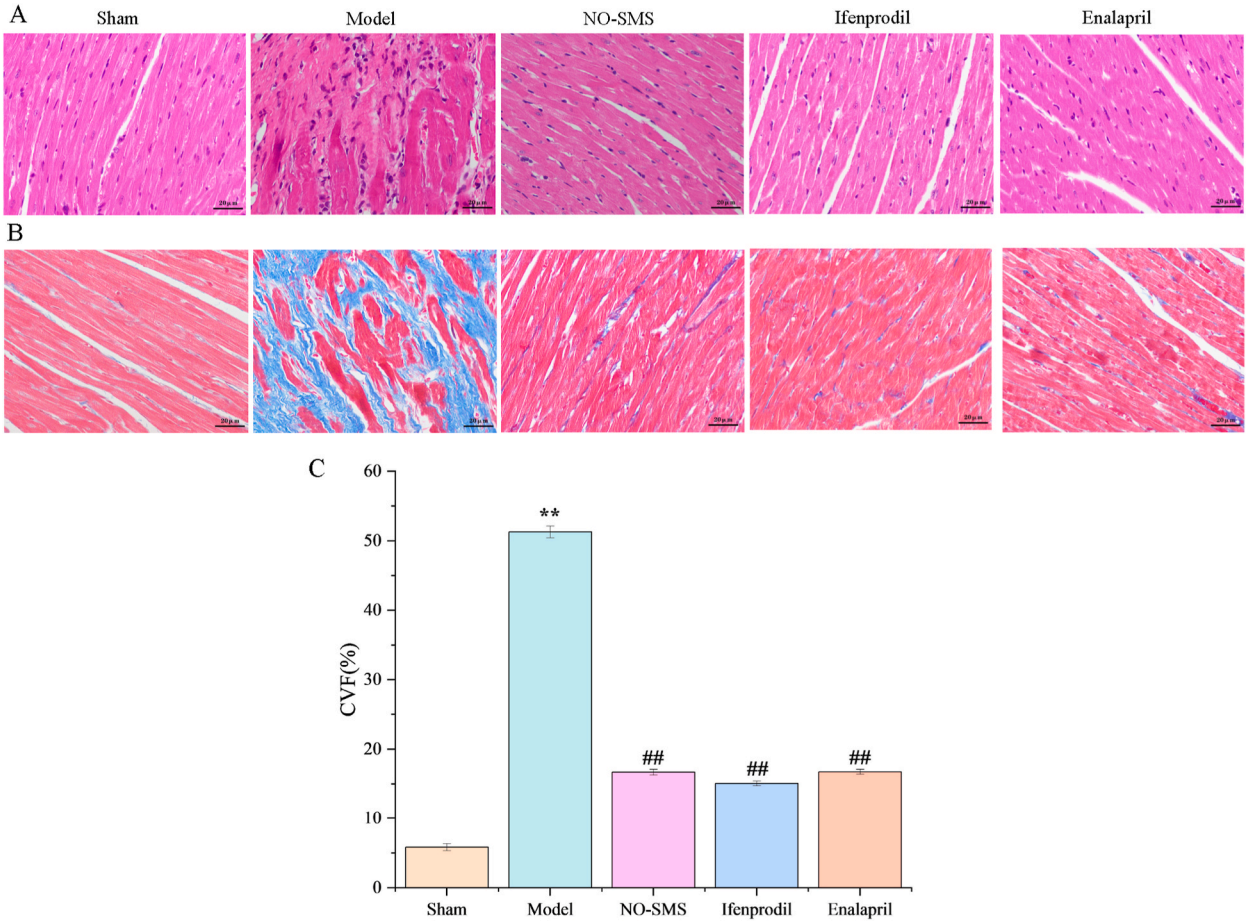

Fig. 2. Histopathological changes of myocardium of rats in each group after drug administration. HE staining: Sham group: clear myocardial transverse lines, dense and neatly arranged fibers, intact cell structure, uniform size, no hypertrophy, centered nucleus, uniform cytoplasmic coloration, no obvious interstitial edema, no obvious abnormalities. Compared with the Sham group, the Model group had broken myofilaments, disorganized fiber arrangement, a large number of myocardial cells were necrotic and disappeared, replaced by proliferating fibrous connective tissue, and there were obvious cell swelling and a large number of inflammatory cell infiltration. Compared with the Model group, NO-SMS, Ifenprodil, and Enalapril myocardial tissue lesions were reduced, and neatly arranged myocardial fibers were seen, with uneven nuclei size and significantly reduced cell swelling, accompanied by partial inflammatory cell infiltration (A); Masson staining showed that the transverse myelopathy was clearly visible in the Sham group, with neatly arranged cells and mild proliferation of scattered collagen fibers in the intervals. Compared with Sham, Model showed that the transverse myocardial striae disappeared, cells were heavily necrotic and replaced by collagen fibers, and the pericellular and interstitial tissues were filled with a large number of collagen fibers. Compared with Model, NO-SMS, Ifenprodil, and Enalapril showed loosening of myocardial fiber structure, some cardiomyocytes were arranged more neatly, and a little collagen fiber hyperplasia was seen around myocytes and interstitial tissue (B); CVF% was shown in the figure, compared with Sham group, $^{**}P < 0.001$; compared with Model, $^{\#\#}P < 0.001$; compared with Ifenprodil group, $P < 0.05$ in NO-SMS group and Enalapril group; compared with NO-SMS group, $P > 0.05$ in Enalapril group (C).

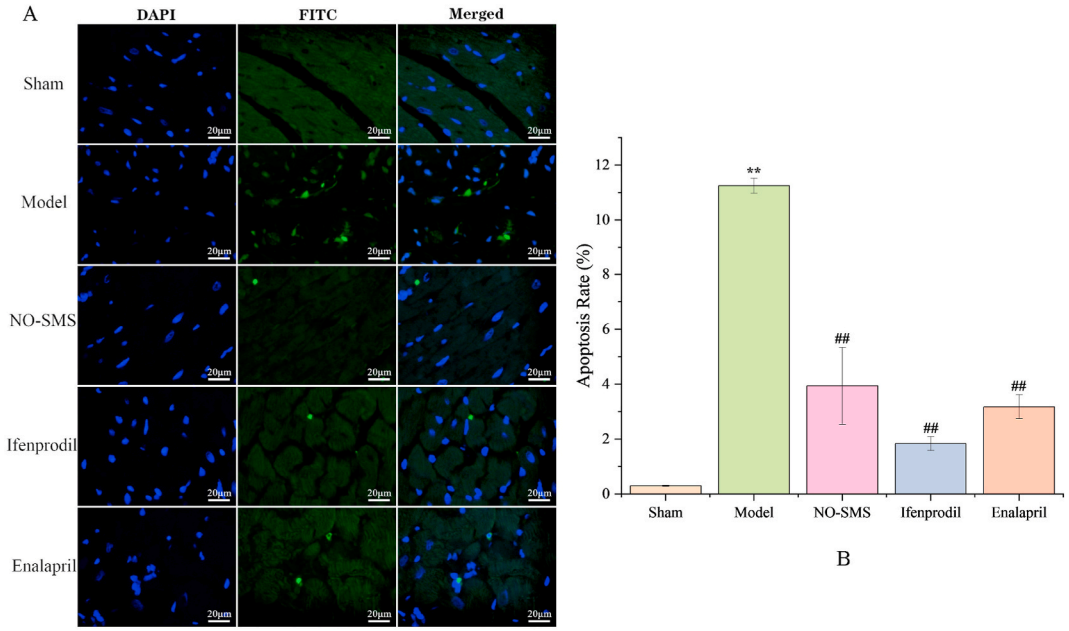

Fig. 3. Apoptosis of rat cardiomyocytes in each group after drug administration. TUNEL staining of rats in each group after 4 weeks of treatment (A); Apoptosis rate of cardiomyocytes in rats in each group (B); Compared with Sham, **P < 0.001; compared with Model, ##P < 0.001; compared with Enalapril group, P > 0.05 in NO-SMS group and Ifenprodil group; compared with NO-SMS group, P < 0.05 in Ifenprodil group.

2.10. Western blotting

The isolated rat left ventricular tissues were placed in liquid nitrogen and then transferred to a −80 °C refrigerator for storage. 50 ± 5 mg myocardial tissues were lysed by using a mixture of RIPA, PMSF, and protein phosphatase inhibitor, and their protein concentration was determined by BCA Protein Assay Kit, while equal amounts of myocardial tissues were boiled for 10 min and separated by SDS-PAGE on 10% gel. The proteins were transferred into the PVDF membrane and then incubated with primary antibodies Caspase-3 (1:500), Caspase-9 (1:500), Caspase-12 (1:2000), Cyt-c (1:5000), Bax (1:5000), Bcl-2 (1:1000), GAPDH (1:2500) overnight at 4 °C. Afterward, the membrane is incubated with the corresponding secondary antibody (1:10 000) for 2 h at room temperature. Immunoreactive bands were visualized by using ECL. The protein signal of the protein band in the membrane is then captured using Image Lab™ software and quantified using the Image J software program.

The logarithmically grown H9c2 cells were removed after 24 h of treatment in the above grouping experimental design, washed three times with pre-cooled PBS at 4 °C; 300 μL of RIPA protein lysate containing PMSF was added and lysed on ice for 30 min; the cell lysate was collected and centrifuged at 12 000 r/min for 10 min at 4 °C; the supernatant was collected and the protein concentration was determined by BCA method and transferred to a 0.5 ml centrifuge tube and set aside at 4 °C. The rest was processed in the same way as rat myocardial tissue.

2.11. qRT-PCR

Total RNA was extracted from myocardial tissue using the HP Total RNA Kit, RNA concentration was detected, and RNA was reversed to cDNA using the HiScript® qRT SuperMix Kit, followed by qRT-PCR using SYBR qPCR Master Mix. The forward and reverse primer sequences used in this study are shown in Table 1. $2^{-\Delta\Delta CT}$ operations were performed on the cycling threshold The relative quantitative expression of mRNA was analyzed.

2.12. Statistical analysis

SPSS 21.0 software was used to statistically analyze the data, and the measurement data were expressed as mean ± standard deviation (x ± s). Those conforming to normal distribution were analyzed by one-way ANOVA, and the LAD method was used for comparison between groups; the Kruskal-Wallis method of rank sum test was used for comparison between groups not conforming to normal distribution; P > 0.05 indicated no statistical difference.

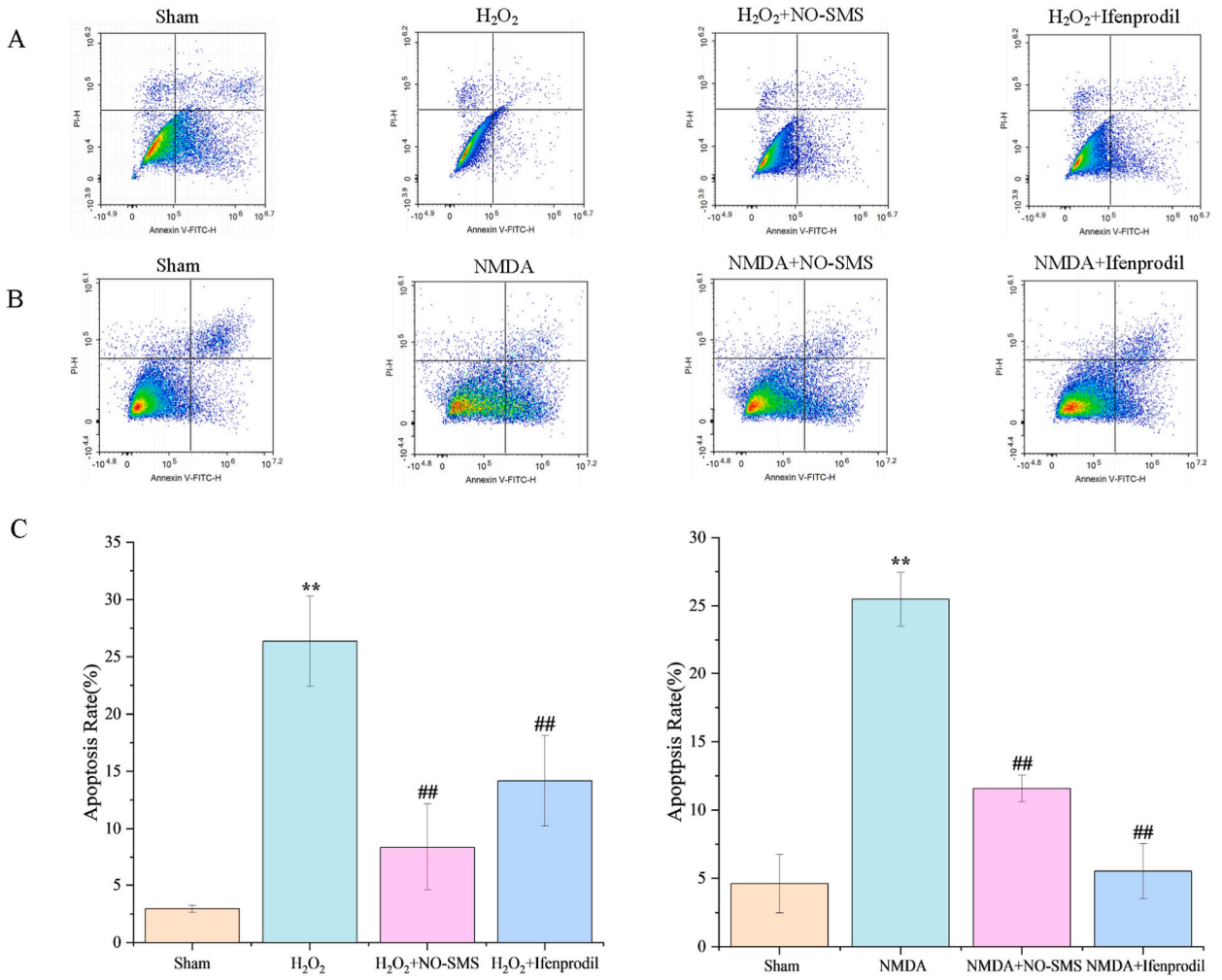

Fig. 4. Apoptosis of H9c2 cardiomyocytes in each group. Annexin V-FITC/PI staining of H9c2 cardiomyocytes in each group treated with H_2O_2 (A); Annexin V-FITC/PI staining of H9c2 cardiomyocytes in each group treated with NMDA (B); Apoptosis rate of H9c2 cardiomyocytes in each group treated with H_2O_2 (C); Apoptosis rate of NMDA-treated H9c2 cardiomyocytes in each group (D); Compared with Sham, $^{**}P < 0.01$; compared with NMDA, $^{\#\#}P < 0.01$; comparison of H_2O_2+NO-SMS group and H_2O_2+Ifenprodil group, $P > 0.05$; comparison of NMDA + NO-SMS group and NMDA + Ifenprodil group, $P < 0.05$.

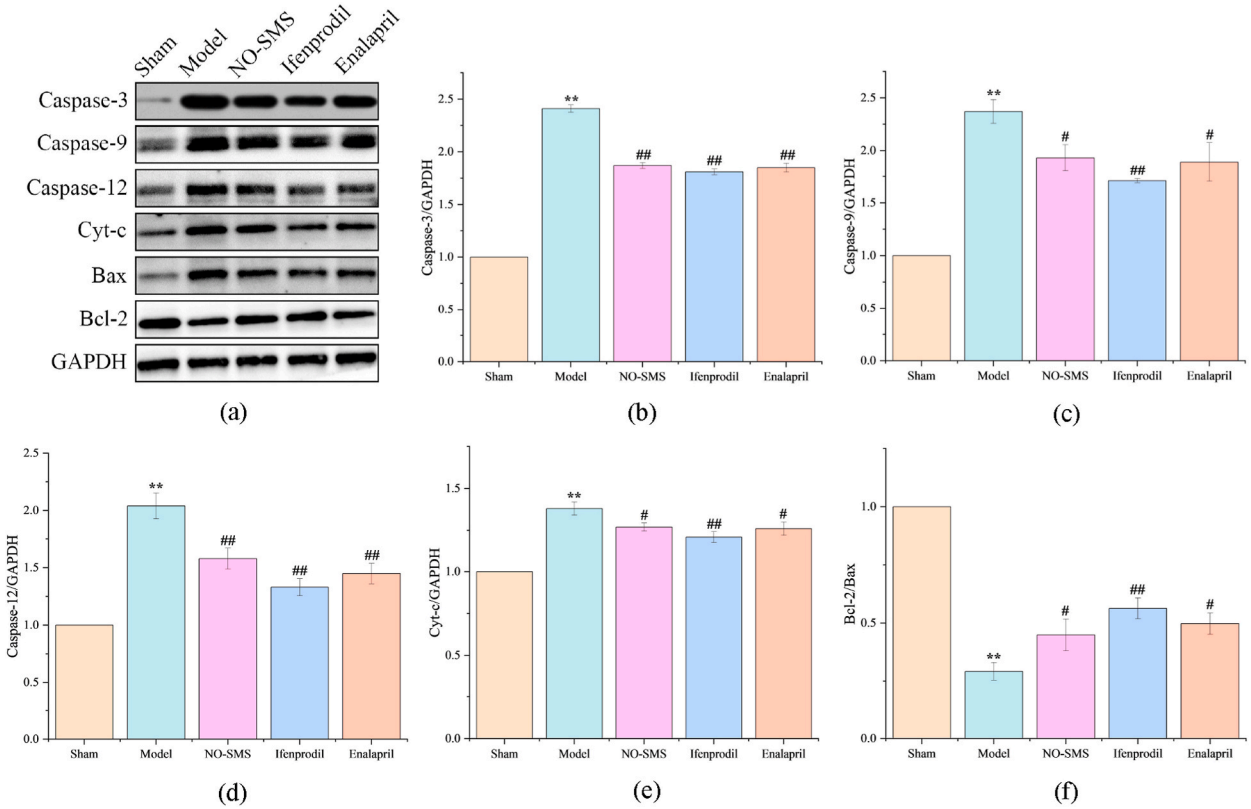

Fig. 5. Expression of apoptosis-related proteins in myocardial tissues. Representative immunoblot bands of various proteins (a); Evaluation of caspase-3, caspase-9, caspase-12, cyt-c, and Bcl-2/Bax levels in each group (b–f); Compared with Sham, $^{**}P < 0.01$; compared with Model, $^{\#}P < 0.05$, $^{\#\#}P < 0.01$.

3. Results

3.1. NO-SMS improves cardiac function in rats with heart failure

The cardiac function of each group before and after administration was measured using echocardiography (Fig. 1 A), and the results showed LVEF and LVFS levels were significantly lower in the remaining groups compared to the Sham group ($P < 0.01$) after administration. After treatment with the NO-SMS formula, the rats' cardiac function was significantly restored, and their LVEF and LVFS levels were significantly higher compared with the Model group ($P < 0.01$). The Ifenprodil group and the Enalapril group had the same significant effect in terms of improvement of cardiac function in rats (Fig. 1 B, C).

3.2. Effect of NO-SMS formula on myocardial pathology and fibrosis in HF rats

NO-SMS formula can reduce the degree of myocardial lesions and delay the process of myocardial fibrosis in HF rats. After H & E staining and Masson staining, we could observe under the light microscope that the extent of myocardial lesions in NO-SMS, Ifenprodil, and Enalapril groups was less severe than that in the Model group, and only a small amount of collagen fiber proliferation was seen in pericellular and interstitial tissues, and cardiomyocytes were more neatly arranged with only some inflammatory cell infiltration (Fig. 2 A, B, C).

3.3. NO-SMS formula reduced apoptosis rate in heart failure rats

The apoptotic rate of cardiomyocytes was reflected by the ratio of the number of green fluorescent cells in the myocardial tissue of HF rats in each group after TUNEL staining. Compared with the Sham group, the myocardial tissue of the Model group showed a large number of cells with positive green fluorescence, and the apoptosis rate of myocardial cells was significantly increased ($P < 0.01$); compared with the Model group, a small number of cells with positive green fluorescence were visible in the myocardial tissue of the

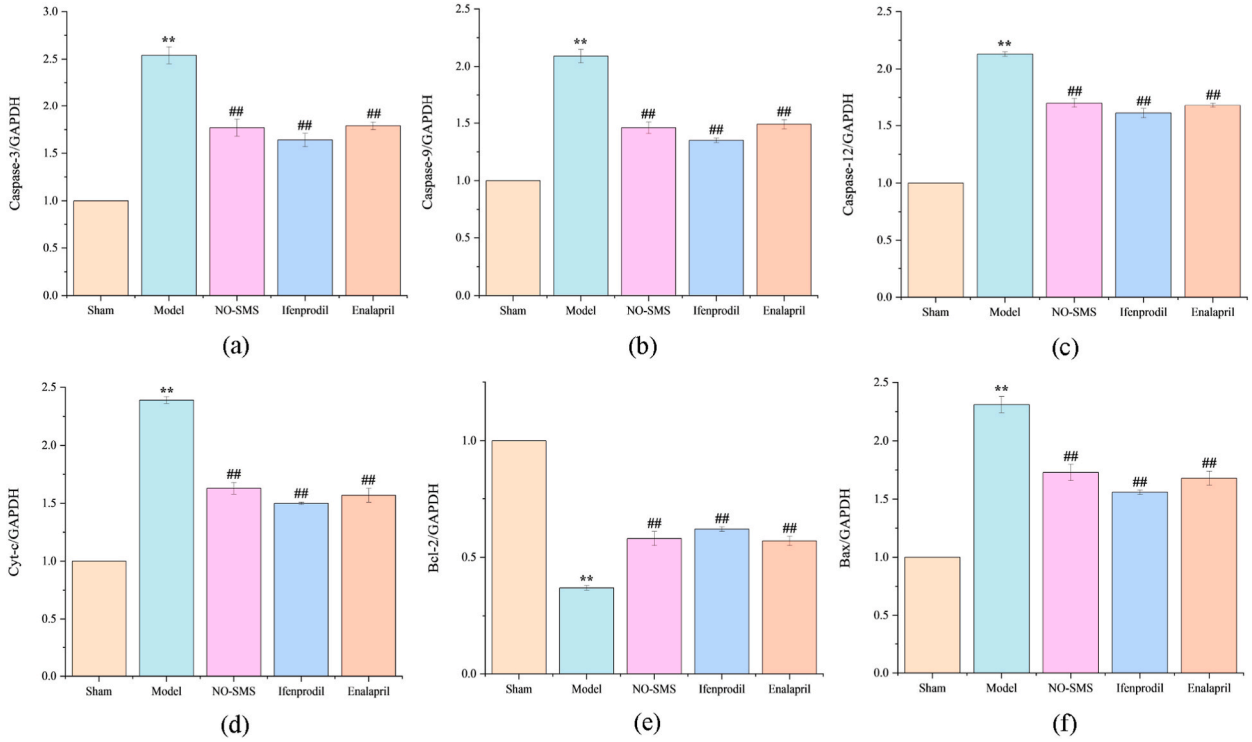

Fig. 6. Apoptosis-related mRNA expression in myocardial tissues. Evaluation of Caspase-3, Caspase-9, Caspase-12, Cyt-c, Bax, Bcl-2 mRNA levels in each group (a–f); Compared with Sham, $^{**}P < 0.01$; compared with Model, $^{\#\#}P < 0.01$.

NO-SMS, Ifenprodil, and Enalapril groups, and the apoptosis rate was significantly reduced ($P < 0.01$). The results reflected a significant anti-apoptotic effect (Fig. 3 A, B).

3.4. NO-SMS formula reduced apoptosis rate of H_2O_2/NMDA-treated H9c2 cardiomyocytes

To further verify the effect of the NO-SMS formula on the apoptosis rate of H_2O_2/NMDA-treated H9c2 cardiomyocytes, we performed the experiment by adding drug-containing serum intervention in each group and then using the Annexin V-FITC/PI for staining and using flow cytometry for scatter plotting and quantitative detection. (Fig. 4 A, B).

The results showed that both H_2O_2 and NMDA induced cardiomyocyte apoptosis ($P < 0.01$). Compared with the H_2O_2 group, the apoptosis rate of cardiomyocytes in the H_2O_2+NO-SMS group ($P < 0.01$) and the H_2O_2+Ifenprodil group ($P < 0.05$) was significantly lower. Compared with the NMDA group, the apoptosis rate of cardiomyocytes in the NMDA + NO-SMS group and the NMDA + Ifenprodil group ($P < 0.01$) was significantly lower (Fig. 4 C, D). The above results demonstrated that H_2O_2/NMDA induced apoptosis in H9c2 cardiomyocytes and the addition of NMDAR inhibitor Ifenprodil significantly reduced the apoptosis rate of cardiomyocytes. Meanwhile, the same significant effect could be achieved by using the NO-SMS formula, which suggested that the NO-SMS formula might achieve the inhibitory effect of cardiomyocyte apoptosis by inhibiting the NMDAR pathway.

3.5. NO-SMS formula inhibited apoptosis by reducing apoptosis protein expression and its mRNA level

High expression of Caspase-3, Caspase-9, Caspase-12, Cyt-c, Bax, and other proteins suggested active apoptosis, while elevated Bcl-2/Bax ratio suggested inhibition of apoptosis. In our study, apoptosis was assessed by measuring the expression of various proteins and their mRNA levels in the myocardial tissue of HF rats and H_2O_2/NMDA-treated H9c2 cardiomyocytes by Western blotting and qRT-PCR. The results showed that both NO-SMS and Ifenprodil groups decreased the levels of pro-apoptotic proteins and their mRNAs and increased the levels of anti-apoptotic proteins and their mRNAs in myocardial tissue of HF rats and H_2O_2/NMDA-treated H9c2 cardiomyocytes compared with the model group. The results demonstrated that the NO-SMS formula inhibited apoptosis by decreasing apoptotic protein expression (Fig. 5a–f, 7a-f, 9a-f) and its mRNA level (Fig. 6a–f 8a-f, 10a-f).

3.6. NO-SMS reduced Ca^{2+} concentration in myocardial tissue of HF rats and H_2O_2/NMDA-treated H9c2 cardiomyocytes

The activation of the NMDAR signaling pathway leads to the accumulation of large amounts of Ca^{2+}, which resulted in endoplasmic

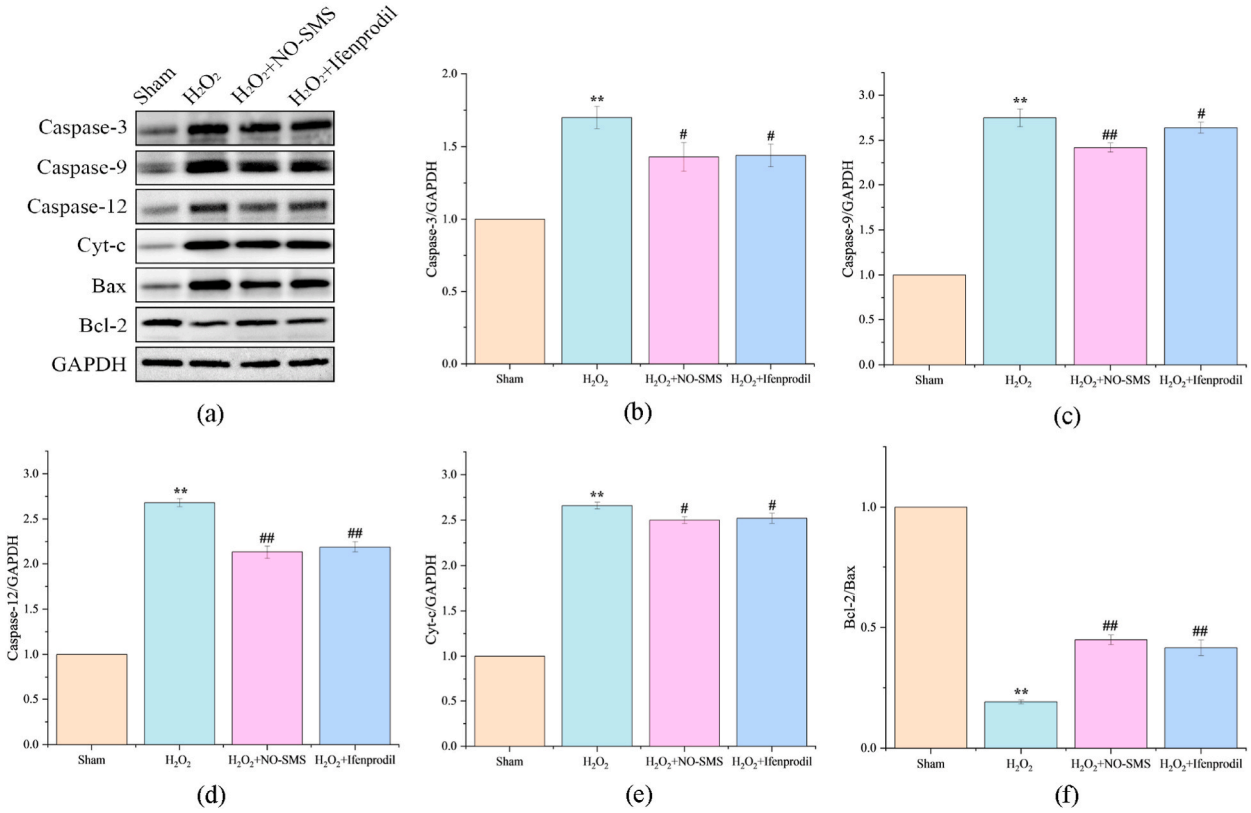

Fig. 7. Expression of apoptosis-related proteins in H_2O_2-treated H9c2 cardiomyocytes. Representative immunoblot bands of various proteins (a); Evaluation of caspase-3, caspase-9, caspase-12, cyt-c, and Bcl-2/Bax levels in each group (b–f); Compared with Sham, $^{**}P < 0.01$; compared with H_2O_2, $^{\#}P < 0.05$, $^{\#\#}P < 0.01$.

reticulum stress and thus apoptosis. In this study, we measured the Ca^{2+} concentration in myocardial tissues of HF rats and H_2O_2/NMDA-treated H9c2 cardiomyocytes by ELISA to verify that NO-SMS inhibited the activation of the NMDAR pathway to reduce Ca^{2+} concentration. The results showed that both NO-SMS formula and Ifenprodil groups significantly reduced the Ca^{2+} concentration in myocardial tissue of HF rats and H_2O_2/NMDA-treated H9c2 cardiomyocytes compared with Model group ($P < 0.01$), and the difference between the administration groups was not statistically significant ($P > 0.05$) (Fig. 11 a-c). These results further suggested that the NO-SMS formula inhibited the accumulation of Ca^{2+} concentration by regulating the activation of the NMDAR signaling pathway, thereby achieving inhibition of apoptosis.

3.7. NO-SMS reduced ROS concentration in myocardial tissue of HF rats and H_2O_2/NMDA-treated H9c2 cardiomyocytes

In this study, we measured the ROS concentration in myocardial tissues of HF rats and H_2O_2/NMDA-treated H9c2 cardiomyocytes by ELISA to verify that NO-SMS inhibited the activation of the NMDAR pathway to reduce ROS concentration. The results showed that both the NO-SMS formula and Ifenprodil groups significantly reduced the ROS concentration in myocardial tissue of HF rats and H_2O_2/NMDA-treated H9c2 cardiomyocytes compared with the Model group ($P < 0.01$), and the difference between the administration groups was not statistically significant ($P > 0.05$). (Fig. 12 a-c).

4. Discussion

NO-SMS formula, a combination of traditional Chinese medicines, has proven its effectiveness in treating HF and improving clinical symptoms in HF patients in clinical applications. In the present study, we investigated the pathological mechanism of the NO-SMS formula for HF through in vivo and in vitro cellular experiments. Our experimental data demonstrates the three factors, including myocardial ischemic changes caused by ligation of the anterior descending branch of the coronary artery, hypoxic necrosis induced by H2O2 in H9c2 cells in vitro, and NMDAR signaling pathway activated in H9c2 cells in vitro by NMDA, all promote the development of cell apoptosis, ultimately leading to the further development of heart failure. However, through the intervention of the NO-SMS formula, it can play a similar role as NMDAR inhibitor in blocking the activation of the NMDAR signaling pathway. NO-SMS

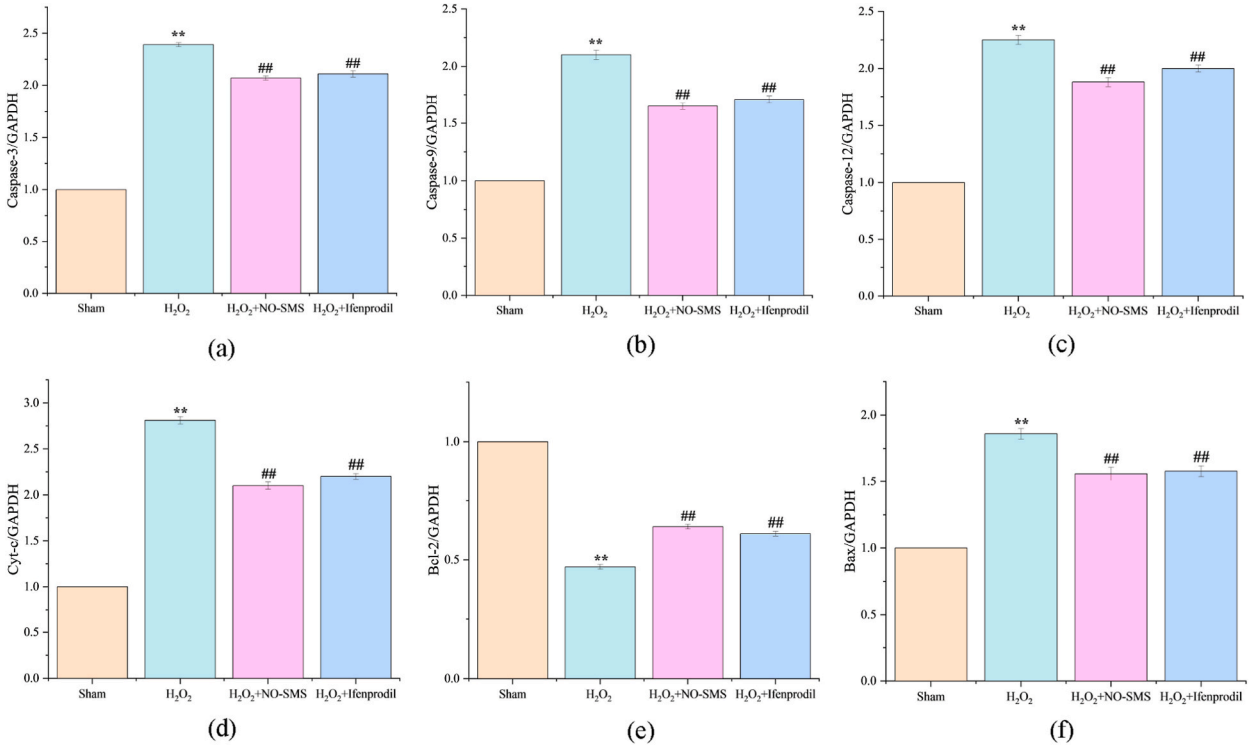

Fig. 8. Apoptosis-related mRNA expression in H_2O_2-treated H9c2 cardiomyocytes. Evaluation of Caspase-3, Caspase-9, Caspase-12, Cyt-c, Bax, Bcl-2 mRNA levels in each group (a–f); Compared with Sham, $^{**}P < 0.01$; compared with H_2O_2, $^{\#\#}P < 0.01$.

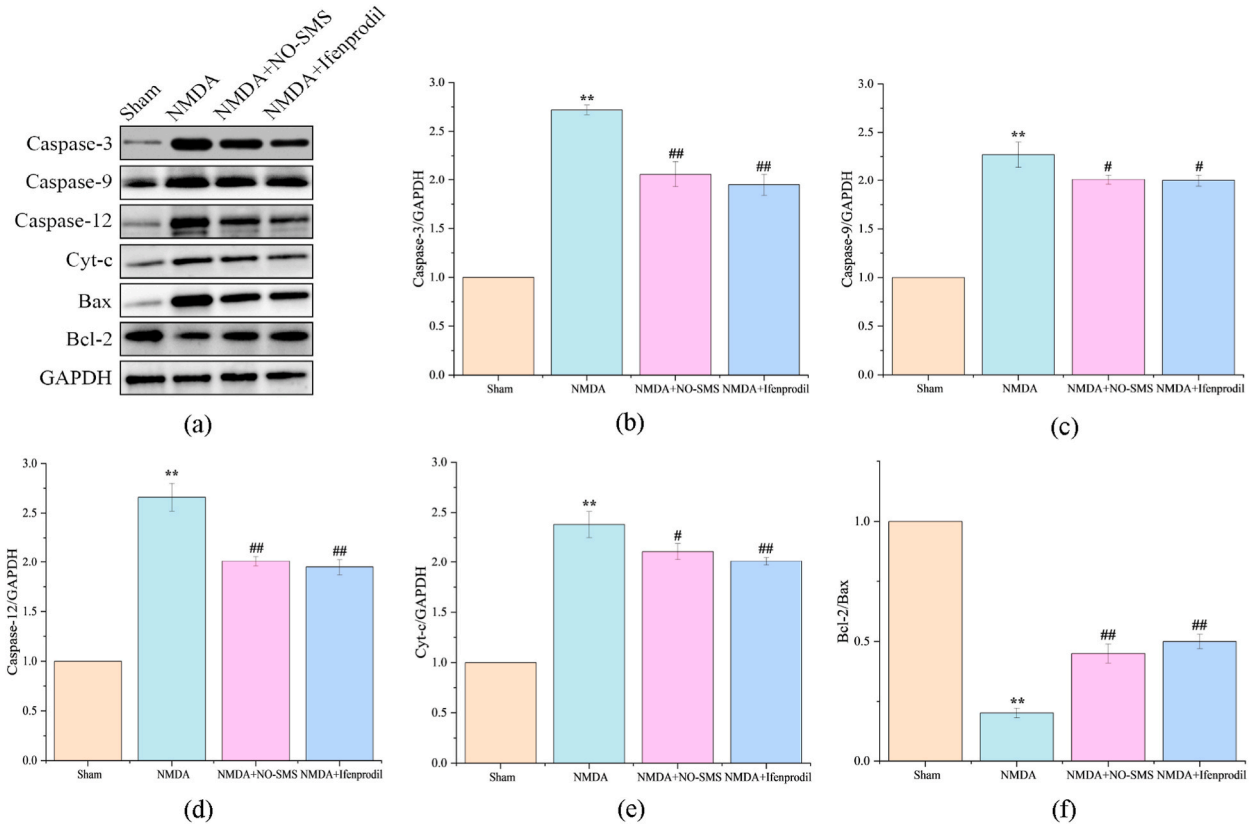

Fig. 9. Expression of apoptosis-related proteins in NMDA-treated H9c2 cardiomyocytes. Representative immunoblot bands of various proteins (a); Evaluation of caspase-3, caspase-9, caspase-12, cyt-c, and Bcl-2/Bax levels in each group (b–f); Compared with NMDA, $^{**}P < 0.01$; compared with NMDA, $^{\#}P < 0.05$, $^{\#\#}P < 0.01$.

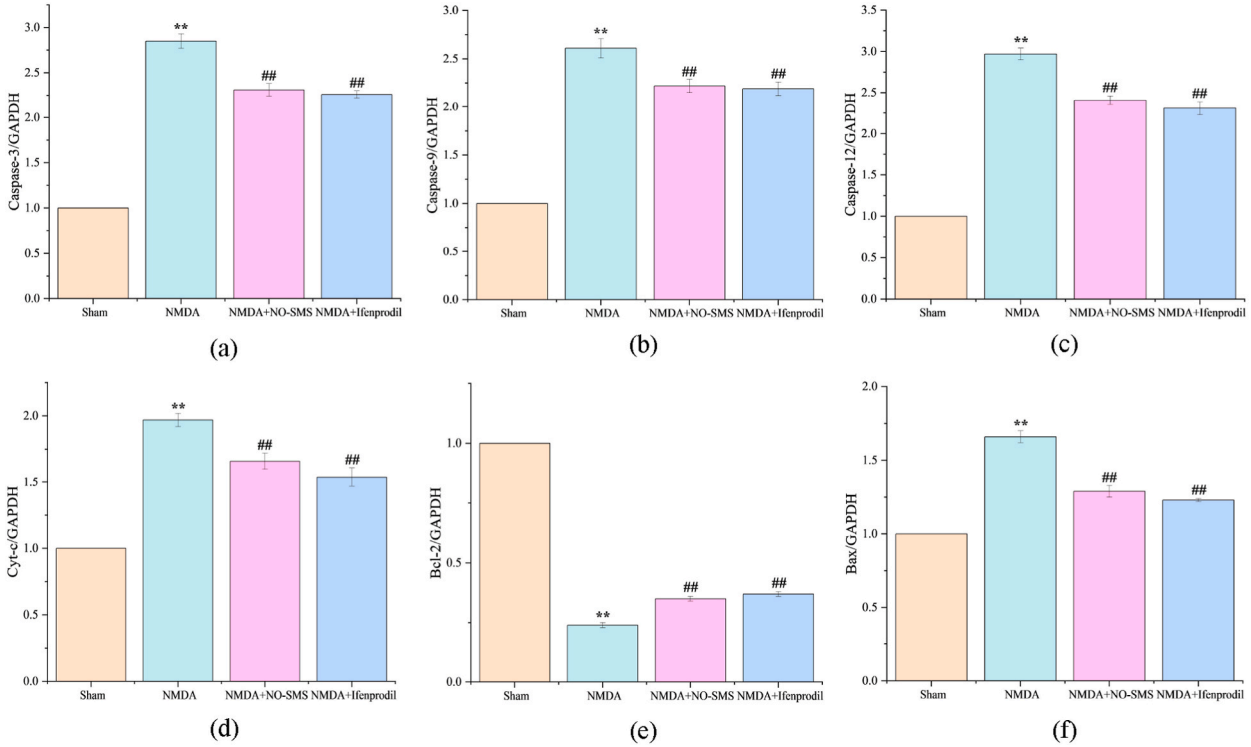

Fig. 10. Apoptosis-related mRNA expression in NMDA-treated H9c2 cardiomyocytes. Evaluation of Caspase-3, Caspase-9, Caspase-12, Cyt-c, Bax, Bcl-2 mRNA levels in each group (a–f); Compared with Sham, $^{**}P < 0.01$; compared with NMDA, $^{\#\#}P < 0.01$.

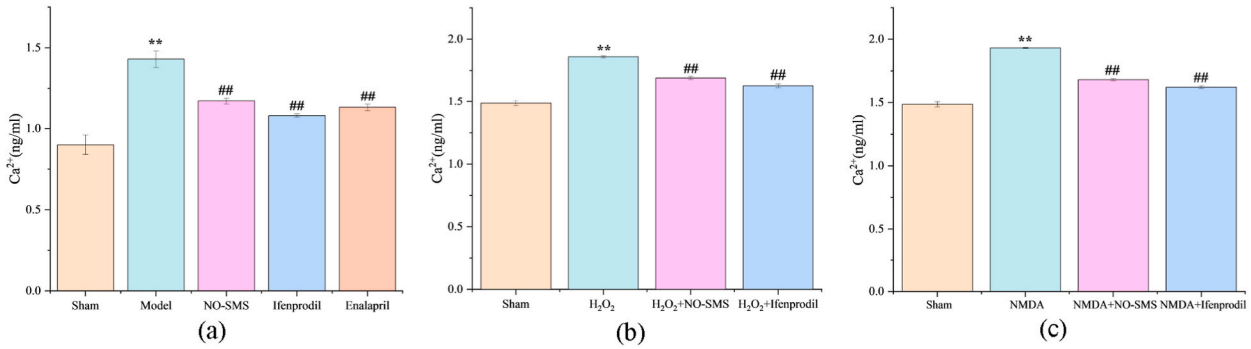

Fig. 11. Ca^{2+} concentration of myocardial tissue and H9c2 cardiomyocytes in each group. Ca^{2+} concentration of myocardial tissue in each group (a); Ca^{2+} concentration of H9c2 cardiomyocytes treated with H_2O_2 in each group (b); Ca^{2+} concentration of H9c2 cardiomyocytes treated with NMDA in each group (c). Compared with Sham, $^{**}P < 0.01$; compared with Model (H_2O_2/NMDA), $^{\#\#}P < 0.01$.

formula inhibits the onset of endoplasmic reticulum stress by reducing intracellular concentration of Ca^{2+} and ROS, thus inhibiting the occurrence of apoptosis by inhibiting the expression of caspase-3, caspase-9, caspase-12, Cyt-c, and Bax and other apoptotic proteins. Thus, the results of our analysis suggested that the NO-SMS formula inhibited apoptosis and delayed the development of ventricular remodeling by modulating the NMDAR signaling pathway to some extent, thereby reducing the incidence of heart failure.

Myocardial apoptosis is an important cause of post-infarction HF and an important factor in the expansion of myocardial infarction, which not only affects the size of myocardial infarction but also aggravates the development of ventricular remodeling. Unlike cell necrosis, apoptosis proceeds in an orderly and controlled manner without loss of cell membrane integrity and release of intracellular material [11]. The two most prominent apoptotic pathways exist, including the exogenous (death receptor-mediated apoptosis) signaling pathway, and the endogenous (mitochondria-mediated apoptosis) signaling pathway, in which the mitochondrial apoptotic signaling pathway functions mainly by regulating the Bcl-2 protein family, and its main mechanism is to control the permeability of the mitochondrial membrane as a way to regulate the release of Cyt-c [12]. Although these two signaling pathways leading to apoptosis are not identical, they are ultimately activated by the same caspase family of apoptosis execution signaling pathways to complete apoptosis [13].

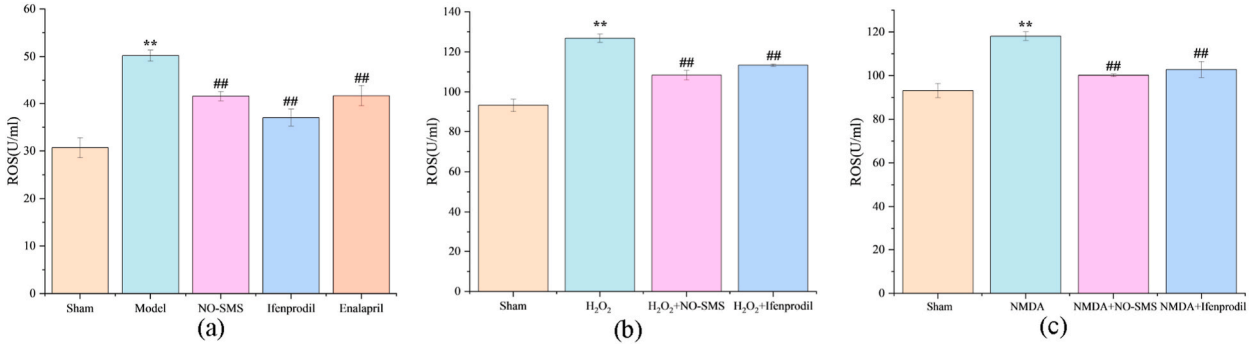

Fig. 12. ROS concentration of myocardial tissue and H9c2 cardiomyocytes in each group. ROS concentration of myocardial tissue in each group (a); ROS concentration of H9c2 cardiomyocytes treated with H_2O_2 in each group (b); ROS concentration of H9c2 cardiomyocytes treated with NMDA in each group (c). Compared with Sham, $^{**}P < 0.01$; compared with Model (H_2O_2/NMDA), $^{\#\#}P < 0.01$.

In contrast, NMDAR, an important ionotropic glutamate receptor, requires glycine (or D-serine) and glutamate (or aspartate) binding to GluN1 and GluN2 subunits [35], respectively, for its activation in the NMDAR signaling pathway, and it is also characterized by Mg^{2+} voltage-dependent blockade, as evidenced by the fact that the NMDAR ion channel is blocked by Mg^{2+} at a membrane potential of approximately −70 mV, and its activation is subject to membrane depolarization [36,37]. When the ligand binds to NMDAR, the ligand-binding domain then closes like a clamshell, and the transmembrane ion channel opens, which in turn mediates the inward flow of Ca^{2+}, Na^{+}, and outward flow of K^{+}, and the relative permeability of Ca^{2+} is 10 times higher than that of Na^{+} [15,38]. When myocardial ischemia occurs, ATP is significantly reduced, and the transport and metabolism of glutamate and glycine are impaired and accumulate outside the cell membrane, and the accumulated glutamate first activates AMPAR, leading to Na^{+} inward flow and cell membrane depolarization, relieving the blocking effect of Mg^{2+} on NMDAR channels under physiological conditions [18], while when NMDAR is overactivated it can trigger the apoptotic program.

The activation by NMDAR signaling pathways, which greatly increases Ca^{2+} permeability, will induce further depolarization of cell membranes and inward flow [14], Liu ZY et al. found that Ca^{2+} levels in isolated ischemic SD rat hearts rose after 30 min and that ischemic myocardial Ca^{2+} was significantly elevated by the addition of NMDA, suggesting that NMDAR activity enhances cardiomyocyte Ca^{2+} inward flow in the presence of irreversible myocardial ischemic injury [17]. When the NMDA receptor pathway is open in the presence of sustained activation, large amounts of Ca^{2+} enter the cell, causing calcium overload [39]and damage to cardiomyocytes via the mitochondrial and endoplasmic reticulum pathways [40]. The large amount of Ca^{2+} in mitochondria opens the mitochondrial permeability transition pore (MPTP) and takes up large amounts of water through higher colloidal osmotic pressure, leading to swelling of mitochondria and rupture of the outer membrane, generating large amounts of ROS [41], resulting in irreversible cellular damage, the release of Cyt-c, decreased Bcl-2 protein expression, dissociation of Bcl-2/Bax heterodimers, increased Bax protein expression, and increased number of Bax/Bax homodimers [42], initiating the apoptotic process [43,44].

Our data confirmed that the use of the NO-SMS formula can significantly enhance the LVEF and LVFS values that were drastically decreased due to myocardial ischemic infarction, and had good effects on enhancing myocardial contractility and cardiac function in rats with ischemic HF, and NO-SMS formula can effectively improve ventricular remodeling as shown by H&E and MASSON staining. Meanwhile, the NO-SMS formula significantly reduced Ca^{2+} and ROS concentrations in HF rat myocardial tissue and H_2O_2/NMDA-treated H9c2 cardiomyocytes, while the NO-SMS formula also down-regulated the expression of pro-apoptotic protein Bax activation and caspase cascade caused by ischemia, oxidative stress, and NMDA injury, decreased Cyt-c release, and up-regulated the expression of inhibitory expression of the apoptotic protein Bcl-2, which is consistent with the results obtained after using the NMDAR inhibitor Ifenprodil. These data suggest that the NO-SMS formula inhibits the activation of the NMDAR signaling pathway, reduces the massive inward flow of Ca^{2+} and the accumulation of ROS, and then inhibits the high expression of related apoptotic proteins, thereby inhibiting apoptosis and delaying the occurrence of ventricular remodeling, providing an effective theoretical basis for the clinical NO-SMS formula to improve the clinical symptoms of heart failure patients and reduce the rehospitalization rate (Fig. 13).

5. Conclusion

In summary, excessive activation of the NMDAR signaling pathway can aggravate ventricular remodeling and apoptosis to further develop heart failure. NO-SMS can inhibit the activation of the NMDAR signaling pathway, reduce the massive Ca^{2+} inward flow and ROS production, and inhibit the expression of the caspase cascade, thus inhibiting myocardial apoptosis and slowing down ventricular remodeling. Therefore, acting on the NMDAR signaling pathway through NO-SMS may be an effective way to treat heart failure and improve patients' clinical symptoms.

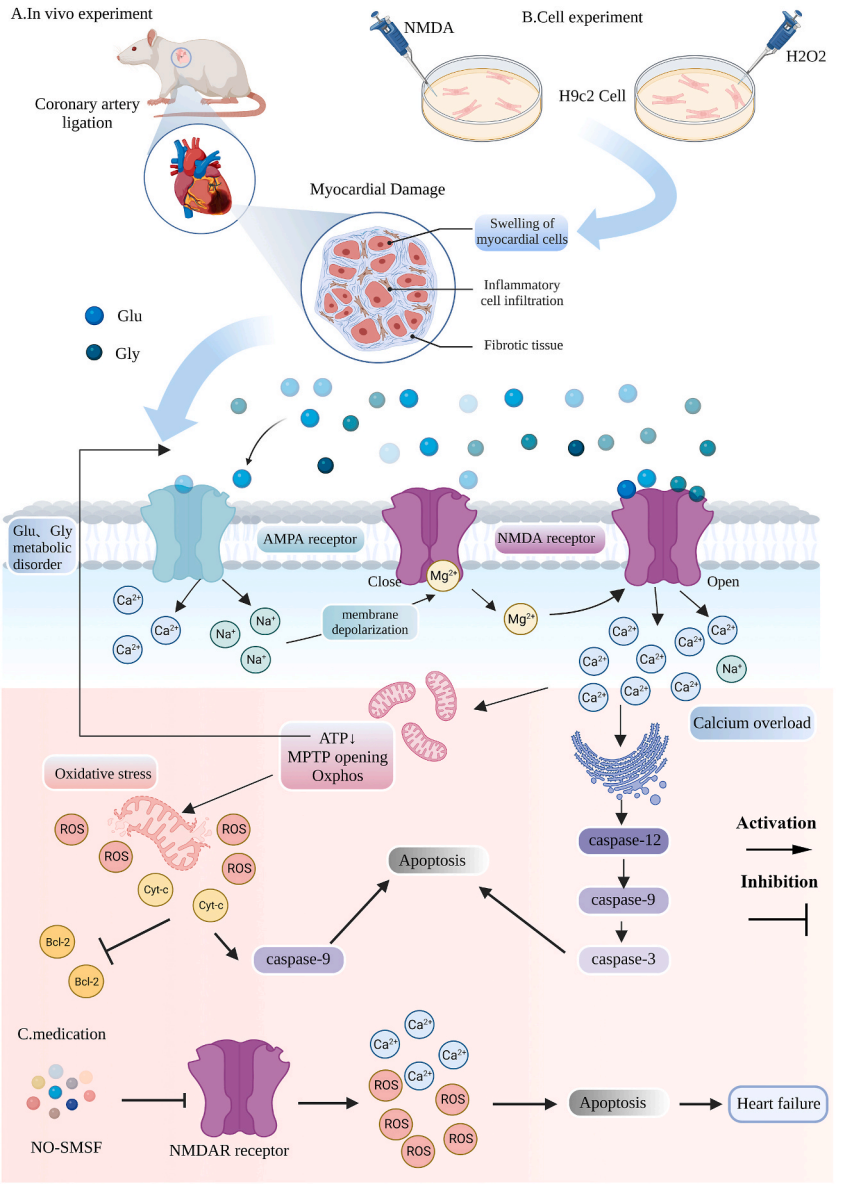

Fig. 13. Mechanism of action diagram. A list of abbreviations: Glu: glutamate; Gly: glycine; AMPA: α-amino-3-hydroxy-5-methyl-4-isoxazole-propionic-acid; NMDA: N-Methyl-D-Aspartate; ATP: Adenosine triphosphate; MPTP: mitochondrial permeability transition pore; ROS: reactive oxygen species; NO-SMS: New Optimized Sheng-Mai-San.

Author contribution statement

Yazhu Hou: Conceived and designed the experiments; Performed the experiments; Analyzed and interpreted the data; Wrote the paper.

Zixun He: Performed the experiments; Analyzed and interpreted the data; Wrote the paper.

Tongyan Zhang; Shuai Wang: Conceived and designed the experiments.

Yixiao Han: Performed the experiments; Analyzed and interpreted the data.

Xianliang Wang; Jingyuan Mao: Contributed reagents, materials, analysis tools or data.

Data availability statement

Data will be made available on request.

Declaration of competing interest

The authors declare that they have no known competing financial interests or personal relationships that could have appeared to influence the work reported in this paper.

Acknowledgments

This research project was supported by National Natural Science Foundation of China [81904150], the Ministry of Education of the People's Republic of China "Program for Innovative Research Team in University" [No. IRT_16254] and Traditional Chinese Medicine & Integrated Traditional Chinese and Western Medicine Project of Tianjin health commission and administration of TCM [No. 2017002].

References

[1] S.S. Virani, A. Alonso, H.J. Aparicio, et al., Heart disease and stroke statistics-2021 update: a report from the American heart association, Circulation 143 (8) (2021) e254–e743, https://doi.org/10.1161/cir.0000000000000950.
[2] A. Groenewegen, F.H. Rutten, A. Mosterd, et al., Epidemiology of heart failure, Eur. J. Heart Fail. 22 (8) (2020) 1342–1356, https://doi.org/10.1002/ejhf.1858.
[3] H. Aghajanian, T. Kimura, J.G. Rurik, et al., Targeting cardiac fibrosis with engineered T cells, Nature 573 (7774) (2019) 430–433, https://doi.org/10.1038/s41586-019-1546-z.
[4] A. González, E.B. Schelbert, J. Díez, et al., Myocardial interstitial fibrosis in heart failure: biological and translational perspectives, J. Am. Coll. Cardiol. 71 (15) (2018) 1696–1706, https://doi.org/10.1016/j.jacc.2018.02.021.
[5] P. Rossignol, A.F. Hernandez, S.D. Solomon, et al., Heart failure drug treatment, Lancet (London, England) 393 (10175) (2019) 1034–1044, https://doi.org/10.1016/s0140-6736(18)31808-7.
[6] N.G. Frangogiannis, Cardiac fibrosis: cell biological mechanisms, molecular pathways and therapeutic opportunities, Mol. Aspect. Med. 65 (2019) 70–99, https://doi.org/10.1016/j.mam.2018.07.001.
[7] B. Zhang, S. Mao, X. Liu, et al., MiR-125b inhibits cardiomyocyte apoptosis by targeting BAK1 in heart failure, Mol. Med. 27 (1) (2021) 72, https://doi.org/10.1186/s10020-021-00328-w.
[8] F.L. Johnson, Pathophysiology and etiology of heart failure, Cardiol. Clin. 32 (1) (2014) 9–19, https://doi.org/10.1016/j.ccl.2013.09.015, vii.
[9] M. Liao, Q. Xie, Y. Zhao, et al., Main active components of Si-Miao-Yong-An decoction (SMYAD) attenuate autophagy and apoptosis via the PDE5A-AKT and TLR4-NOX4 pathways in isoproterenol (ISO)-induced heart failure models, Pharmacol. Res. 176 (2022), 106077, https://doi.org/10.1016/j.phrs.2022.106077.
[10] Y.F. Li, K.G. Cornish, K.P. Patel, Alteration of NMDA NR1 receptors within the paraventricular nucleus of hypothalamus in rats with heart failure, Circ. Res. 93 (10) (2003) 990–997, https://doi.org/10.1161/01.Res.0000102865.60437.55.
[11] P.M. Kang, S. Izumo, Apoptosis in heart: basic mechanisms and implications in cardiovascular diseases, Trends Mol. Med. 9 (4) (2003) 177–182, https://doi.org/10.1016/s1471-4914(03)00025-x.
[12] W.N. Lu, F.P. Zheng, D.W. Lai, et al., Xuezhikang reduced renal cell apoptosis in streptozocin-induced diabetic rats through regulation of Bcl-2 family, Chin. J. Integr. Med. 22 (8) (2016) 611–618, https://doi.org/10.1007/s11655-015-2050-4.
[13] E. Teiger, V.D. Than, L. Richard, et al., Apoptosis in pressure overload-induced heart hypertrophy in the rat, J. Clin. Invest. 97 (12) (1996) 2891–2897, https://doi.org/10.1172/jci118747.
[14] H. Wu, B.S. Ng, G. Thibault, Endoplasmic reticulum stress response in yeast and humans, Biosci. Rep. 34 (4) (2014), https://doi.org/10.1042/bsr20140058.
[15] V. Vyklicky, M. Korinek, T. Smejkalova, et al., Structure, function, and pharmacology of NMDA receptor channels, Physiol. Res. 63 (Suppl 1) (2014) S191–S203, https://doi.org/10.33549/physiolres.932678.
[16] S.J. Dumas, G. Bru-Mercier, A. Courboulin, et al., NMDA-type glutamate receptor activation promotes vascular remodeling and pulmonary arterial hypertension, Circulation 137 (22) (2018) 2371–2389, https://doi.org/10.1161/circulationaha.117.029930.
[17] Z.Y. Liu, S. Hu, Q.W. Zhong, et al., N-Methyl-D-Aspartate receptor-driven calcium influx potentiates the adverse effects of myocardial ischemia-reperfusion injury ex vivo, J. Cardiovasc. Pharmacol. 70 (5) (2017) 329–338, https://doi.org/10.1097/fjc.0000000000000527.
[18] T. Dohi, K. Morita, T. Kitayama, et al., Glycine transporter inhibitors as a novel drug discovery strategy for neuropathic pain, Pharm. Therap. 123 (1) (2009) 54–79, https://doi.org/10.1016/j.pharmthera.2009.03.018.
[19] D.P. Del Re, D. Amgalan, A. Linkermann, et al., Fundamental mechanisms of regulated cell death and implications for heart disease, Physiol. Rev. 99 (4) (2019) 1765–1817, https://doi.org/10.1152/physrev.00022.2018.
[20] G.W. Moe, J. Marín-García, Role of cell death in the progression of heart failure, Heart Fail. Rev. 21 (2) (2016) 157–167, https://doi.org/10.1007/s10741-016-9532-0.
[21] F. Hu, S. Zhang, X. Chen, et al., MiR-219a-2 relieves myocardial ischemia-reperfusion injury by reducing calcium overload and cell apoptosis through HIF1α/NMDAR pathway, Exp. Cell Res. 395 (1) (2020), 112172, https://doi.org/10.1016/j.yexcr.2020.112172.
[22] C. Zhang, T.W. Syed, R. Liu, et al., Role of endoplasmic reticulum stress, autophagy, and inflammation in cardiovascular disease, Front. Cardiovas. Med. 4 (2017) 29, https://doi.org/10.3389/fcvm.2017.00029.
[23] W. Mughal, R. Dhingra, L.A. Kirshenbaum, Striking a balance: autophagy, apoptosis, and necrosis in a normal and failing heart, Curr. Hypertens. Rep. 14 (6) (2012) 540–547, https://doi.org/10.1007/s11906-012-0304-5.
[24] M. Jougasaki, Cardiotrophin-1 in cardiovascular regulation, Adv. Clin. Chem. 52 (2010) 41–76, https://doi.org/10.1016/s0065-2423(10)52002-x.
[25] S. Treskatsch, M. Shakibaei, A. Feldheiser, et al., Ultrastructural changes associated with myocardial apoptosis, in failing rat hearts induced by volume overload, Int. J. Cardiol. 197 (2015) 327–332, https://doi.org/10.1016/j.ijcard.2015.06.067.
[26] Z.Y. Zhang, X.L. Wang, S. Wang, et al., Discussion about the mechanism of optimized pulse-engendering powder against myocardial fibrosis in chronic heart failure based on network pharmacology and molecular docking technology, Henan Traditional Chinese Medicine 42 (7) (2022) 1032–1039, https://doi.org/10.16367/j.issn.1003-5028.2022.07.0222.
[27] X.L. Wang, Y. Yuan, J.Y. Mao, et al., A single-case crossover randomized controlled study to Optimized New Sheng-mai Powder formula with western medicine in the treatment of chronic heart failure, 56, J. Tradit. Chin. Med. 21 (2015) 1849–1853, https://doi.org/10.13288/j.11-2166/r.2015.21.013.
[28] Z.K. Li, Effective observation on treating CHF with Xin Shengmai San plus western medicine, Clinical Journal of Chinese Medicine 8 (28) (2016) 20–22.
[29] Z.G. Wu, Comparison of the effects of Optimized New Shengmai Powder and New Shengmai Powder in the treatment of chronic heart failure with Qi deficiency, blood stasis and water retention, Modern Diagnosis and Treatment 28 (22) (2017) 4136–4137.
[30] X.F. He, B.L. Tang, X. Wang, et al., Efficacy analysis of Yiqi Huoxue Lishui Formula for heart failure in coronary heart disease due to qi deficiency blood stasis and fluid-retention, Moder. Chin. Clin. Med. 27 (3) (2020) 9–12.
[31] Y.X. Han, Y.Z. Hou, H.F. Yan, et al., Advances in N-methyl-Daspartate receptor signaling pathway and mechanism of the pathway-mediated apoptosis, Acta Acad. Med. Sin. 37 (10) (2020) 1176–1182.
[32] H.Y. Chen, L.X. Lou, Y.Z. Zhao, et al., Effects of qidan lixin pill on miR-133a/TGF-β1/CTGF signaling pathway in left ventricle myocardial tissue of myocardial infarction, J. Tradit. Chin. Med. 59 (20) (2018) 1771–1776.

[33] K.K. Liu, S. Wang, A.M. Wu, et al., The mechanism of QidanlixinPill in alleviating myocardial apoptosis in rats with myocardial infarction, Chin. J. Med. Cardio-Cerebrovas. Dis. 19 (3) (2021) 423–427.
[34] B. Shi, Y. Huang, J. Ni, et al., Qi Dan Li Xin pill improves chronic heart failure by regulating mTOR/p70S6k-mediated autophagy and inhibiting apoptosis, Sci. Rep. 10 (1) (2020) 6105, https://doi.org/10.1038/s41598-020-63090-9.
[35] D.A. Sibarov, S.M. Antonov, Calcium-dependent desensitization of NMDA receptors, Biochem. Biokhimiia 83 (10) (2018) 1173–1183, https://doi.org/10.1134/s0006297918100036.
[36] P. Montes de Oca Balderas, Flux-Independent NMDAR signaling: molecular mediators, cellular functions, and complexities, Int. J. Mol. Sci. 19 (12) (2018), https://doi.org/10.3390/ijms19123800.
[37] E.R. Kandel, Y. Dudai, M.R. Mayford, The molecular and systems biology of memory, Cell 157 (1) (2014) 163–186, https://doi.org/10.1016/j.cell.2014.03.001.
[38] I. Stojic, I. Srejovic, V. Zivkovic, et al., The effects of verapamil and its combinations with glutamate and glycine on cardiodynamics, coronary flow and oxidative stress in isolated rat heart, J. Physiol. Biochem. 73 (1) (2017) 141–153, https://doi.org/10.1007/s13105-016-0534-0.
[39] J. Krebs, L.B. Agellon, M. Michalak, Ca(2+) homeostasis and endoplasmic reticulum (ER) stress: an integrated view of calcium signaling, Biochem. Biophys. Res. Commun. 460 (1) (2015) 114–121, https://doi.org/10.1016/j.bbrc.2015.02.004.
[40] C. Nastos, K. Kalimeris, N. Papoutsidakis, et al., Global Consequences of Liver Ischemia/reperfusion Injury, Oxidative Medicine and Cellular Longevity, vol. 2014, 2014, 906965, https://doi.org/10.1155/2014/906965.
[41] M.L. Guo, P. Periyasamy, K. Liao, et al., Cocaine-mediated downregulation of microglial miR-124 expression involves promoter DNA methylation, Epigenetics 11 (11) (2016) 819–830, https://doi.org/10.1080/15592294.2016.1232233.
[42] P. Kumar, I.K. Coltas, B. Kumar, et al., Bcl-2 protects endothelial cells against gamma-radiation via a Raf-MEK-ERK-survivin signaling pathway that is independent of cytochrome c release, Cancer Res. 67 (3) (2007) 1193–1202, https://doi.org/10.1158/0008-5472.Can-06-2265.
[43] P. Chen, W.L. Gu, M.Z. Gong, et al., shRNA-mediated silencing of hTERT suppresses proliferation and promotes apoptosis in osteosarcoma cells, Cancer Gene Ther. 24 (8) (2017) 325–332, https://doi.org/10.1038/cgt.2017.22.
[44] S.J. Repas, N.S. Saad, P.M.L. Janssen, et al., Memantine, an NMDA receptor antagonist, prevents thyroxin-induced hypertension, but not cardiac remodeling, J. Cardiovasc. Pharmacol. 70 (5) (2017) 305–313, https://doi.org/10.1097/fjc.0000000000000521.